# Numerical and Experimental Analysis of Aerofoil for electric -Manned Air Vehicle (e-MAV)

[1]MOHAMMED DANISH, [2]NEETESH KUMAR, [3]S SATISH REDDY,[4]RAMESH KUMAR S C

[1,2,3]UG Students, School Of Mechanical Engineering, REVA University, Bengaluru

[4]Assistant Professor, School Of Mechanical Engineering, REVA University, Bengaluru

***Abstract:* -** In this work, NACA M2 aerofoil was analyzed. The analysis carried out was by varying wind velocities and angles of attack of NACA M2 aerofoil model. Analysis is performed experimentally in the wind tunnel testing facility and similarly CFD analysis is performed to obtain various parameters such as Cl (coefficient of lift), Cd (coefficient of drag) & Cp (coefficient of pressure).We have fabricated NACA M2 aerofoil model using composite material and its size considering the experimental setup dimensions. The natures of the graphs of comparative analysis were found to be similar. Similarly, for NACA 0008 aerofoil we have performed CFD analysis and obtained velocity and pressure contour. On the basis of CFD and experimental results we can conclude that NACA M2 aerofoil has better coefficient of lift and coefficient of drag, on this basis we can say that NACA M2 aerofoil comparatively can be a substitute for various e-MAV application.

**Keywords-** Coefficient of drag, Coefficient of lift, Computational Fluid Dynamics, NACA M2 , NACA 0008

## I.INTRODUCTION

The Electric Manned Aerial Vehicle (e-MAV) is an aircraft with human aboard. e-MAV has various applications such as surveillance, product delivery, agricultural, photography and defense. The aerofoil plays an important role in flight and control of the eMAV. Referring to the literature review it is found that NACA M2 aerofoil hasn't yet been used for the e-MAV applications. NACA 0008 which is used for the various applications is compared experimentally and analytically. NACA M2 aerofoil is tested with the help of Wind Tunnel Testing facility. ANSYS is used to obtain pressure and velocity contours which eventually is used to obtain coefficient of drag and coefficient of lift. Aerofoil Nomenclature **-** The geometry of every airfoil can be described by certain terms such as Leading edge, Trailing edge, Chord Length, Camber, Mean Camber line, Thickness and Angle of Attack.

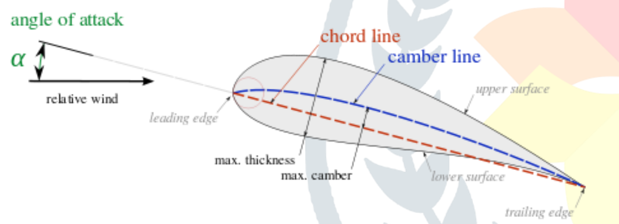


**Figure 1:** Nomenclature of Aerofoil

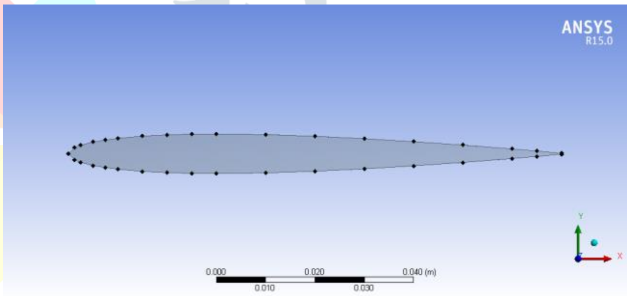


**Figure 2:** Aerofoil of NACA 0008

Figure 2 shows the aerofoil profile of NACA 0008.The coordinates were imported from NACA websites into excel sheets and later imported into ANSYS via .txt file. The geometry is formed and aerofoil profile is generated.

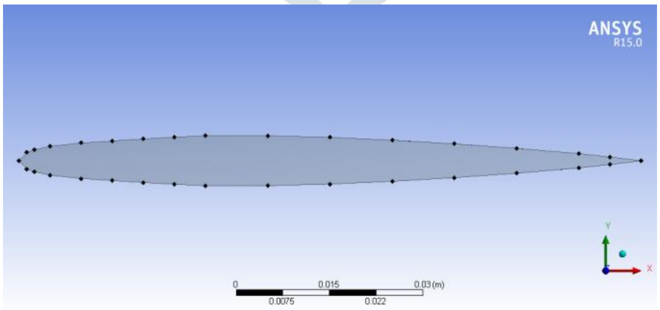


**Figure 3:** Aerofoil of NACA M2

Figure 3 shows the aerofoil profile of NACA M2. Based on the research conducted as a part of the literature survey it's decided to work on estimating the possibility of using an aerofoil for an e-MAV. We accomplished this by simulating the airflow around NACA 0008 and NACA M2.Because of more scope is involved to carry out research of these aerofoil due to good stability conditions.

## II. OBJECTIVE

- To determine co-efficient of drag and co-efficient lift for NACA 0008 aerofoil numerically.
- To determine co-efficient of drag and co-efficient lift for NACA M2 aerofoil numerically and experimentally.

# III. METHODOLOGY

### 3.1 Numerical and experimental

The theoretical method involves testing of our NACA M2 model. The model will have varied holes with extended steel tubes. The wind tunnel testing facility is utilized; our model is placed in the testing facility. Under various speeds the model is put under test, the parameters such as coefficient of drag and coefficient of lift are calculated. The manometric values for different holes present on the model are noted down i.e. $h_i$ & $h_\infty$. Further calculations to obtain parameters such as $C_n$, $C_{p,}$ $C_l$ for various angles of attack and velocity of wind. We later plot graphs such as Cl v/s x, Cd v/s x, Cl v/s AOA (Angle of Attack) & Cd v/s AOA.

hi (in cm) - manometric port in cm
h∞ (in cm) - static pressure in cm
$\Delta h = hi - h\infty$ (manometric port pressure difference)
$\Delta p = \rho h \Delta h$
$Cp = \Delta p / q\infty$
x - Location of the pressure points on aerofoil
c= Chord length
$q_\infty = \frac{1}{2}\rho_{air}\, V_\infty^{2}$
Cd- coefficient of drag
Cl – coefficient of lift
$Cd = Cn \sin\alpha$
$Cl = Cn \cos\alpha$, α-angle of attack.

**Figure 4:** Low speed wind tunnel facility

### 3.2 ANSYS Part

It involves ANSYS. Initially we import co-ordinate points from the NACA site to obtain accurate profile. The coordinates obtained are accordingly customized corresponding to the required standards of ANSYS. Profile is created by importing this .txt file. All the points are joined and surface is created. As it is external flow it is advised to create an external boundary to visualize the flow of fluid. The fluid we consider here is air.

We use Boolean option to separate the external boundary with the aerofoil. This is done to ensure proper meshing on the boundary. Meshing is done to obtain precise results after applying boundary conditions. The input for this model analysis is air.
Variation of parameters such as velocity of air and angle of attack is done. The velocity of air considered in metre per second is 25m/s. The varying angle of attacks in degree are 3°, 6°,9°, 12° & 15 °.

We have increased the size of the boundary and meshing of the boundary too much better refined comparatively. NACA 0008 for 25m/s we have obtained contours at angle of attack 3°, 6°,9°, 12° & 15 °. Similarly for NACA M2 too we obtained the same.

### 3.3 Model Description

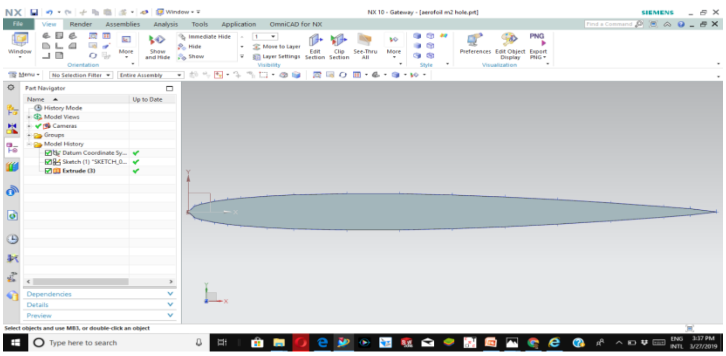

**Figure 5:** 3D Model of NACA M2

Figure 5 shows a 3D model of NACA M2 designed in Solid works. The description of the testing model is standard profile of NACA M2 aerofoil profile with its total length 593mm,chord length 217mm and the thickness 25.75mm. Pitot tubes are connected from the inner side of the model with respective marked points/holes on the surface of the model. Figure 6 shows the fabricated model of NACA M2 along with aluminium supports which are used in experimental analysis.

- Mould material – Mild Steel
- Hardener Resin – LY550
- Glass Fibre – Satin weave 300GSM & chop stand mat 600GSM
- Steel Tubes – 15Tubes of 1.5mm diameter
- Total weight - 2kg
- Pressure port - 15

**Figure 6:** Fabricated Model Of The Wing.

### 3.4 WIND TUNNEL TESTING

The model fabricated is according to the testing facility dimensions. The aerofoil has various ports present in it and respective connections are provided to obtain manometric readings at the facility. The wind speeds of 25m/s are blown over the model.
The manometric readings for different angles of attack are noted down from -15 degrees to 15 degrees.

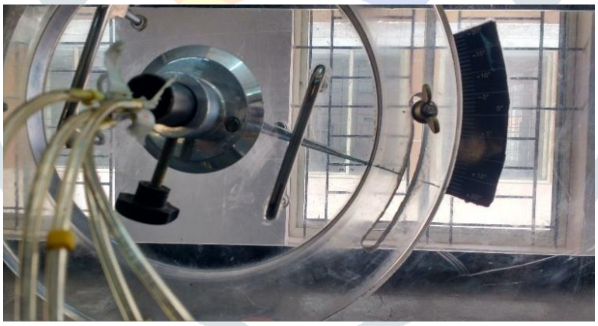

**Figure 7:** Model at 15° Angle Of Attack

Figure 7 shows the experimental setup of the wind tunnel testing along with the model of NACA M2 at 15 degree of angle of attack. To obtain parameters mainly such as coefficient of lift (cl), coefficient of drag (cd) angles of attacks are changed. The tables are obtained for various angles of attack and wind velocities. The calculations for further steps are done using formulas to calculate coefficient of pressure, x/c ratio i.e. port distance from leading edge to chord length.

$h_i$ = manometric port in cm
$h_\infty$ = static pressure in cm
$\Delta h$ = manometric port pressure difference
$\Delta p$ = $\rho h \Delta h$
$C_p$ = $\Delta p / q_\infty$
x = Location of the pressure points on aerofoil
c = chord length
$q\infty$ = $\frac{1}{2} \rho_{atm} v_\infty^2 = 0.5*1.225*25*25 = 382.8125$
Cd = coefficient of drag
Cl = coefficient of lift
Cd = $Cn \sin\alpha = 1.9946* \sin(3) = 0.104$
Cl = $Cn \cos\alpha = -.0516* \cos(3) = -0.051$

**Table No 1:** 3° Angle Of Attack

| Port no | $h_i$ | $h_o$ | Δh | $c_p$ |
|---|---|---|---|---|
| 1 | 31.3 | 27.8 | -0.035 | -0.89692 |
| 2 | 31.3 | 27.8 | -0.035 | -0.89692 |
| 3 | 30.9 | 27.8 | -0.031 | -0.79441 |
| 4 | 30.5 | 27.8 | -0.027 | -0.69191 |
| 5 | 30.4 | 27.8 | -0.026 | -0.66628 |
| 6 | 29.7 | 27.8 | -0.019 | -0.4869 |
| 7 | 28.9 | 27.8 | -0.011 | -0.28189 |
| 8 | 27.9 | 27.8 | -0.001 | -0.02563 |
| 9 | 28.5 | 27.8 | -0.007 | -0.17938 |
| 10 | 28.7 | 27.8 | -0.009 | -0.23064 |
| 11 | 28.9 | 27.8 | -0.011 | -0.28189 |
| 12 | 29.1 | 27.8 | -0.013 | -0.33314 |
| 13 | 29 | 27.8 | -0.012 | -0.30752 |
| 14 | 28.9 | 27.8 | -0.011 | -0.28189 |
| 15 | 24.5 | 27.8 | 0.033 | 0.845668 |

**Table No 2:** coefficient of pressure values

| Port No | $C_{pl}$ | $C_{pu}$ | d(x/c) | $\Delta c_n$ |
|---|---|---|---|---|
| 1 | -0.28189 | -0.89692 | 0.156 | 0.095945 |
| 2 | -0.30752 | -0.89692 | 0.066 | 0.038901 |
| 3 | -0.33314 | -0.79441 | 3.952 | 1.822952 |
| 4 | -0.28189 | -0.69191 | 0.00561 | 0.0023 |
| 5 | -0.23064 | -0.66628 | 0.008 | 0.003485 |
| 6 | -0.17938 | -0.4869 | 0.0244 | 0.007503 |
| 7 | -0.02563 | -0.28189 | 0.092 | 0.023576 |
| | | | Cn | 1.994662 |

**Table No 3:** -3° Angle of Attack

| Port no | $h_i$ | $h_o$ | Δh | $C_p$ |
|---|---|---|---|---|
| 1 | 28.6 | 27.9 | -0.007 | -0.17938 |
| 2 | 29.4 | 27.9 | -0.015 | -0.38439 |
| 3 | 29.45 | 27.9 | -0.0155 | -0.39721 |
| 4 | 29.5 | 27.9 | -0.016 | -0.41002 |
| 5 | 29.5 | 27.9 | -0.016 | -0.41002 |
| 6 | 29.4 | 27.9 | -0.015 | -0.38439 |
| 7 | 29 | 27.9 | -0.011 | -0.28189 |
| 8 | 28.2 | 27.9 | -0.003 | -0.07688 |
| 9 | 28.8 | 27.9 | -0.009 | -0.23064 |
| 10 | 29.3 | 27.9 | -0.014 | -0.35877 |
| 11 | 29.8 | 27.9 | -0.019 | -0.4869 |
| 12 | 29.9 | 27.9 | -0.02 | -0.51253 |
| 13 | 30.1 | 27.9 | -0.022 | -0.56378 |
| 14 | 30.4 | 27.9 | -0.025 | -0.64066 |
| 15 | 26.5 | 27.9 | 0.014 | 0.358768 |

**Table No 4:** coefficient of pressure values

| Ports | $C_{pl}$ | $C_{pu}$ | d(x/c) | $\Delta C_n$ |
|---|---|---|---|---|
| 1 | -0.64066 | -0.17938 | 0.156 | -0.07196 |
| 2 | -0.56378 | -0.38439 | 0.066 | -0.01184 |
| 3 | -0.51253 | -0.39721 | 3.952 | -0.45574 |
| 4 | -0.4869 | -0.41002 | 0.00561 | -0.00043 |
| 5 | -0.35877 | -0.41002 | 0.008 | 0.00041 |
| 6 | -0.23064 | -0.38439 | 0.0244 | 0.003752 |
| 7 | -0.07688 | -0.28189 | 0.092 | 0.018861 |
| | | | $C_n$ | -0.51694 |

### 3.5 MESHING

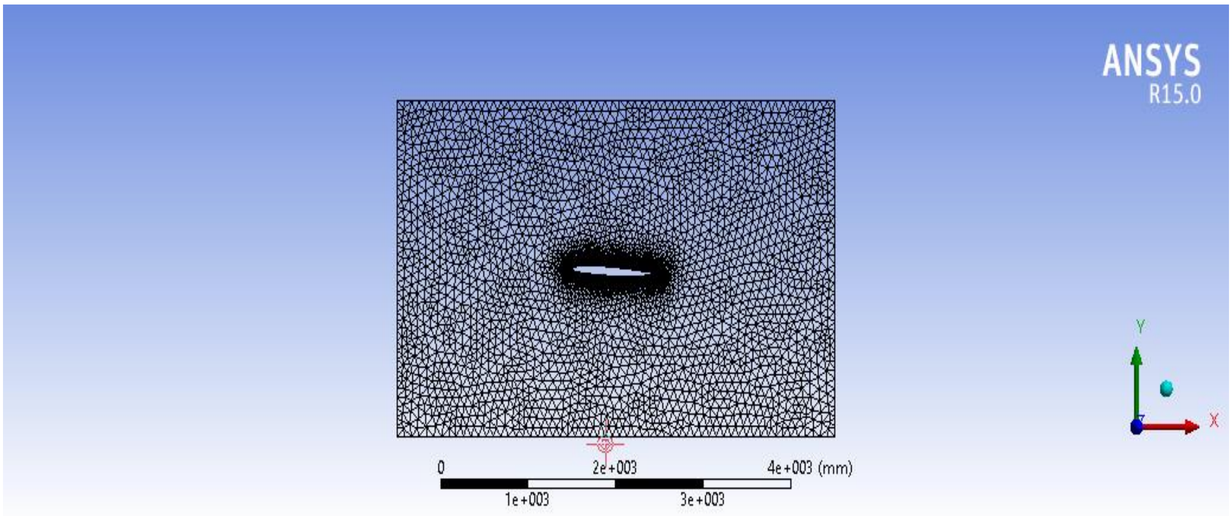


**Figure 8:** Meshing For 3° Angle Of Attack Of NACA M2

The aerofoil point coordinates were imported and the model was meshed for various angles of attack. The boundaries were created similar to the wind tunnel testing facility utilized to obtain values in the theoretical testing of NACA M2 aerofoil.

Table 5: meshing elements for 3 angle of attack

| | |
|---|---|
| **Number of nodes in The mesh** | **20637** |
| **Number of elements in the mesh** | **35042** |
| **Number of iterations for generating mesh** | **1000** |
| **Air density** | **1.225kg-m-3** |

Table 6: meshing elements for -3 angle of attack

| | |
|---|---|
| **Number of nodes in The mesh** | **47247** |
| **Number of elements in the mesh** | **51970** |
| **Number of iterations for generating mesh** | **1000** |
| **Air density** | **1.225kg-m-3** |

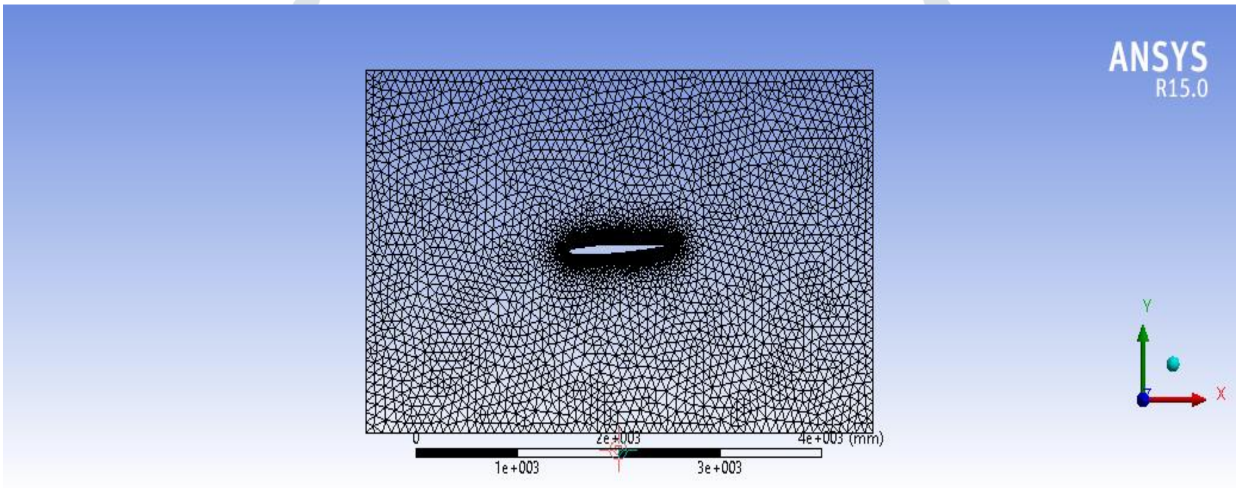


**Figure 9:** Meshing For -3°Angle Of Attack Of NACA M2

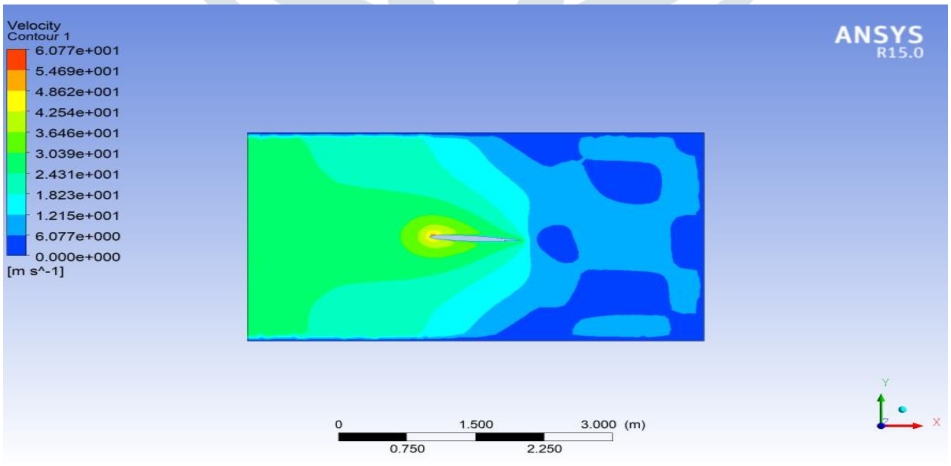


**Figure 10:** Velocity contour for wind 25m/s and 3° angle of attack for NACA M2

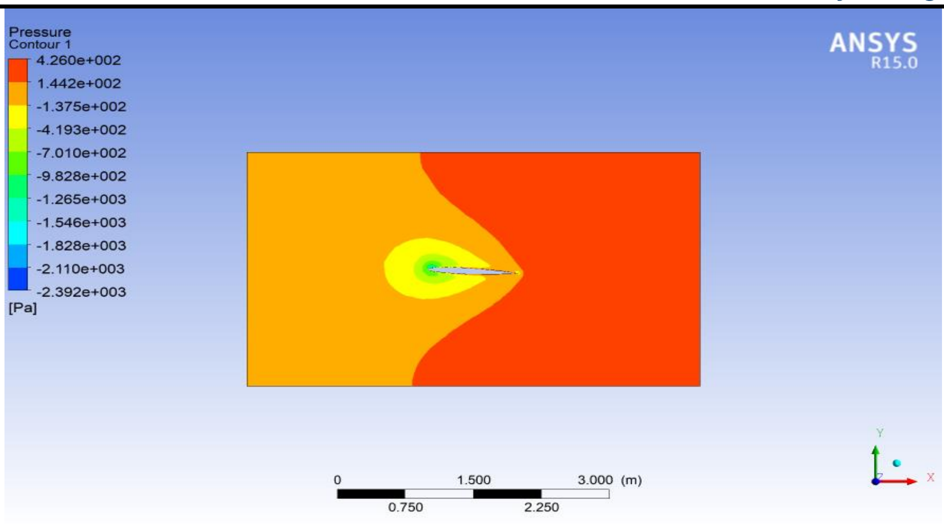


**Figure 11:** Pressure contour for wind 25m/s and 3° angle of attack for NACA M2

The velocity in figure 10 and pressure contours in figure 11 shows us the variation and range of the respective parameters along with the representing colours at the various sites of the aerofoil (here). The detailed version contours help us visualize the variation clearly. We can observe in the pressure contour that the pressure is maximum at the leading edge especially at the lower surface of the aerofoil. It is observed that the due to varied angle of attack the upper surface of the aerofoil is getting lesser effect of pressure due to its lack of direct airflow contact. Similarly, in the detailed velocity contour the effect of wind velocity is maximum at leading edge of the aerofoil and the upper surface due to the virtue of its position experiences lesser velocity effects

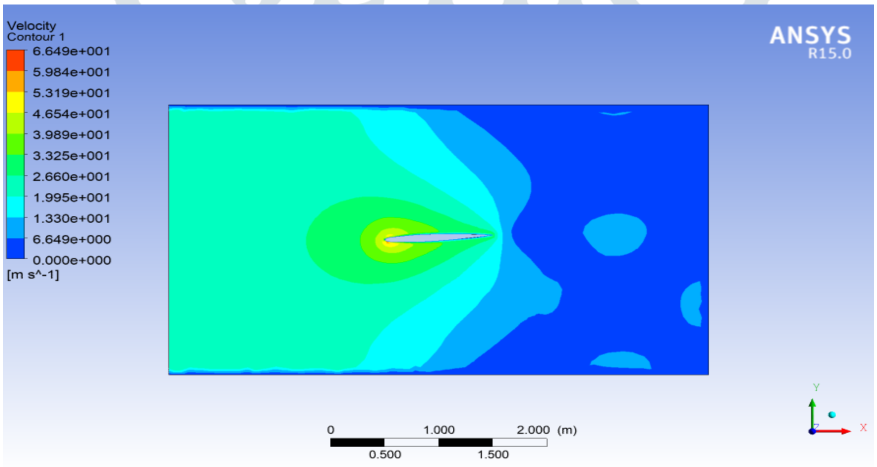


**Figure 12:** Velocity contour for wind 25m/s and -3° angle of attack for NACA M2

Figure 12 shows velocity contour for wind 25m/s and -3 degree angle of attack. We can see the effect of velocity at the leading edge and variation along the profile of the aerofoil.

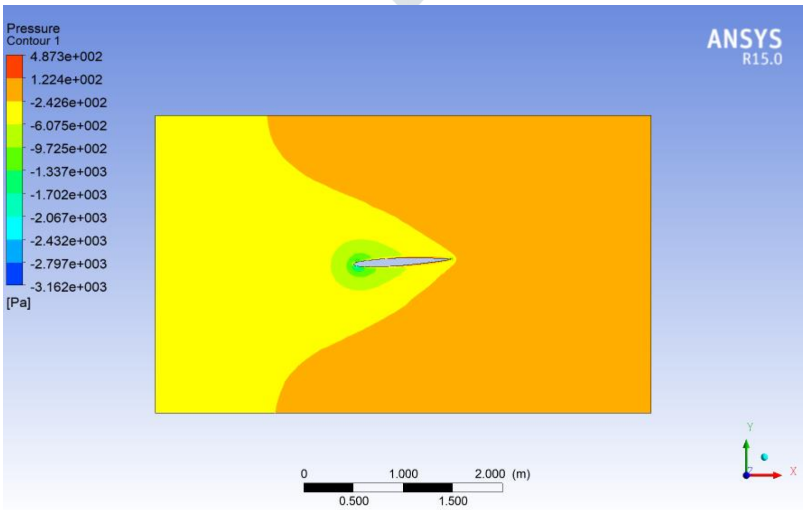


**Figure 13:** Pressure contour for wind 25m/s and -3° angle of attack for NACA M2

Figure 13 shows pressure contour for wind 25m/s and -3 degree angle of attack. We can see the effect of pressure at the leading edge and variation along the profile of the aerofoil.

We can also observe these effects in the detailed contours in figures 16 and figure 17. Later in figure 18 and figure19 the comparative results of the CFD analysis of the NACA M2 aerofoil and the experimental results of the wind tunnel testing.

The graphs are plotted for coefficient of drag and lift on the y axis and the angle of attack on the x axis respectively on two different graphs.

## IV COMPARISON BETWEEN EXPERIMENTAL AND CFD RESULTS

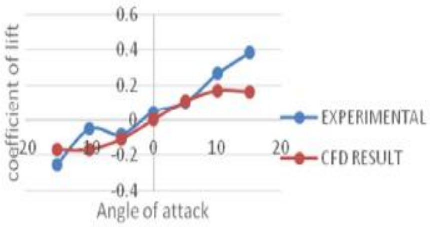


**Figure 14:** Coefficients of Lift v/s angle of attack for 25m/s wind speed

The figure 14 shows us the comparison of CFD result and experimental result for the parameter coefficient of lift against angle of attack. It can be observed that the nature of the graphs that CFD and experimental results' naute matches.

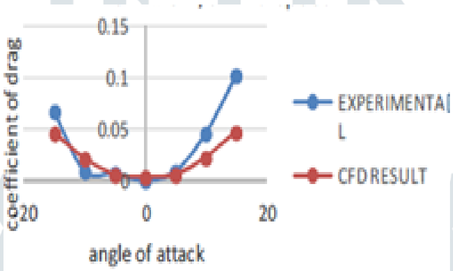


**Figure 15:** Coefficients of Drag v/s angle of attack for 25m/s wind speed

The results are plotted for both ANSYS and wind tunnel for various angles of attack and correspondingly coefficient of lift and coefficient of drag. The nature of the graphs obtained for comparisons for coefficient of lift possessed the same nature of graph and similarly the nature of graph.

## V APPLICATIONS

Symmetric aerofoils are predominantly used in e-MAV's (electric Manned Aerial Vehicle):

Symmetric aerofoils have varied applications but are predominantly used in the e-MAV. As we need large lift and less drag, symmetric aerofoils are useful.

- Reaching remote places: These aerofoils are basically having large flight time thus travelling farther distances where man cannot reach e.g. hilly areas.
- The NACA M2 aerofoils can be used in surveillance over a large area
- The NACA M2 can be used at low values of flow Reynolds number.

## VI CONCLUSION

- The graphs obtained from the comparison from the ANSYS and wind tunnel testing show similar nature of graph
- Lift of NACA M2 IS higher than NACA 0008 and drag of NACA M2 is lower than NACA 0008
- NACA M2 will act as good substitute for NACA 0008 application

## REFERENCES

[1] Şahin, İ, &Acir, A. (2015, February). Numerical and Experimental Investigations of Lift and Drag Performances of NACA 0015 Wind Turbine Airfoil. International Journal of Materials, Mechanics and Manufacturing, 3(1), 22-25.

[2] Eleni, D. C., Athanasios, T. I., &Dionissios, M. P. (2012, March). Evaluation of the turbulence models for the simulation of The flow over a National Advisory Committeefor Aeronautics (NACA) 0012 airfoil. Journal of Mechanical Engineering Research, 4, 100-111.

[3] Kevadiya, M. (2013, May). CFD Analysis of Pressure Coefficient for NACA 4412. International Journal of Engineering Trends and Technology, 4(5), 2041-2043.

[4] Gulzar, O., Gulzar, S., Bhatele, S., &Soni, N. (2014). Impact of Variation in Angle of Attack on NACA 7420 Airfoil in Transonic Compressible Flow Using SpalartAllmaras Turbulence Model. International Journal of Research in Mechanical Engineering and Technology, 4 (2), 35-36.

[5] Marathe, M. S., & Bansode, S. N. (2013). Airfoil Selection of MAV (Miniature Air Vehicle) for Low Reynolds Number. International Journal on Theoretical and Applied Research in Mechanical Engineering, 2 (4), 38-42.

[6] Hossain, M. S., Raiyan, M. F., Akanda, M. N., & Jony, N. H. (2014). A Comparative Flow Analysis of Naca 6409 and Naca 4412 Aerofoil. International Journal of Research in Engineering and Technology, 3 (10), 342- 350.

[7] Ahmed, T., Amin, M. T., Islam, S. R., & Ahmed, S. (2013). Computational Study of Flow around a NACA 0012 Wing Flapped at Different Flap Angles with Varying Mach Numbers. Global Journal of Researches in Engineering General Engineering, 13 (4), 5-15.

[8] Anjali Balani , Tarun Yadav , Appasaheb Malagaudanavar Comparative Cfd Analysis Of Airfoils For Unmanned Aerial Vehicles IJRET: International Journal of Research in Engineering and Technology

[9] Ovais Gulzar, Saqib Gulzar, Sanjay Bhatele, Neelesh Soni Impact of Variation in Angle of Attack on NACA 7420 Airfoil in Transonic Compressible Flow Using SpalartAllmaras Turbulence Model International Journal of Research in Mechanical Engineering & Technology.